An analysis of the heat source contribution of ball screw based on WNN and PSO

Huayang Wu
Jiejing Li
Dunwen Zuo (imit505@nuaa.edu.cn)
Nanjing University of Aeronautics and Astronautics

Research Article

Keywords: ball screw, heat source contribution, wavelet neural network, particle swarm optimization algorithm

Posted Date: May 18th, 2022

DOI: https://doi.org/10.21203/rs.3.rs-1642389/v1

Title

An analysis of the heat source contribution of ball screw based on WNN and PSO

Author names and affiliations

Huayang Wu[1], Jiejing Li[1], Dunwen Zuo[1*]

[1]College of Mechanical and Electrical Engineering, Nanjing University of Aeronautics and Astronautics, Nanjing, China

[*]Correspondent author. Telephone:025-84890249

E-mail address: imit505@nuaa.edu.cn

Acknowledgement

This research is supported by Jiangsu Science and Technology Achievement Conversion Project (No.BA2018093).

Abstract: Fundamentally, the heat source in the ball screw feed system accounts for the thermal behavior of the ball screw. Based on the analysis of the contribution of each heat source in the system to the thermal deformation of the ball screw, this paper sets out to provide a new method for thermal error compensation. It aims to explore the thermal deformation of ball screw and optimize the distribution of heat source contribution so as to provide theoretical guidance for the cooling of ball screw heat source. Firstly, the relationship between heat source and temperature, temperature and thermal deformation is analyzed theoretically, for the sake of illuminating the relationship between heat source and thermal deformation and the further deduction of the implicit mathematical expression of heat source contribution. Secondly, the network model of ball screw thermal deformation and temperature at the heat source is constructed based on wavelet neural network (WNN). Combined with the mathematical analysis results, the explicit mathematical expression of thermal deformation and heat source under this working condition is deduced, and the explicit mathematical expression of heat source contribution is further obtained. After that, keeping the total heat source contribution constant under this working condition, the particle swarm optimization (PSO) algorithm is used to determine the heat source contribution distribution that can minimize the thermal deformation of the ball screw. Finally, the simulation results of ball screw temperature field and thermal deformation before and after optimization are analyzed to examine the rationality and accuracy of the optimization results.

Keywords: ball screw, heat source contribution, wavelet neural network, particle swarm optimization algorithm

An analysis of the heat source contribution of ball screw based on WNN and PSO

Huayang Wu[1], Jiejing Li[1], Dunwen Zuo[1*]

1College of Mechanical and Electrical Engineering, Nanjing University of Aeronautics and Astronautics, Nanjing 210016, China

* Correspondent author. Telephone:025-84890249

E-mail address: imit505@nuaa.edu.cn

Abstract: Fundamentally, the heat source in the ball screw feed system accounts for the thermal behavior of the ball screw. Based on the analysis of the contribution of each heat source in the system to the thermal deformation of the ball screw, this paper sets out to provide a new method for thermal error compensation. It aims to explore the thermal deformation of ball screw and optimize the distribution of heat source contribution so as to provide theoretical guidance for the cooling of ball screw heat source. Firstly, the relationship between heat source and temperature, temperature and thermal deformation is analyzed theoretically, for the sake of illuminating the relationship between heat source and thermal deformation and the further deduction of the implicit mathematical expression of heat source contribution. Secondly, the network model of ball screw thermal deformation and temperature at the heat source is constructed based on wavelet neural network (WNN). Combined with the mathematical analysis results, the explicit mathematical expression of thermal deformation and heat source under this working condition is deduced, and the explicit mathematical expression of heat source contribution is further obtained. After that, keeping the total heat source contribution constant under this working condition, the particle swarm optimization (PSO) algorithm is used to determine the heat source contribution distribution that can minimize the thermal deformation of the ball screw. Finally, the simulation results of ball screw temperature field and thermal deformation before and after optimization are analyzed to examine the rationality and accuracy of the optimization results.

Keywords: ball screw, heat source contribution, wavelet neural network, particle swarm optimization algorithm

0. Introduction

Owing to the constant pursuit of machining quality and efficiency, the requirement of modern manufacturing industry to CNC machining center is high-precision and high-speed machining. The positioning accuracy of the cutting tool mainly depends on the thermal deformation of the ball screw feed system. This is due to the existence of various heat sources such as motor and friction heat, which leads to the thermal deformation of the ball screw and the positioning error between the workpiece and the tool. Many studies indicates that the thermal error accounts for about 40% ~ 70% of the total error of the machine tool [1-2]. The methods of suppressing the thermal error in the ball screw feed system mainly include error avoidance method and error compensation method.

Mitigating the influence of internal heat source on the main body of ball screw is the main means of avoiding error, such as cooling, heat insulation and so on. Zhao et al. [3] designed the cooling plate with the built-in channel of the ball screw and installed it at the heat source. Each

cooling circuit is equipped with a separate oil tank for independent temperature regulation. The establishment of the heat generation model of the heat source, such as the bearing, motor and ball screw nut of the feed shaft, can help accurately match the heat generation rate of each heat source to control the temperature of the inlet and outlet coolant in the cooling system, so as to differentially take away the heat generated in different heat sources and control the temperature of each part. Shi et al. [4] elucidated the relationship between convective heat transfer coefficient and cooling system parameters when the flow velocity of cooling medium is constant. The effects of channel geometry and coolant flow velocity on thermal behavior were investigated with the help of numerical simulation. The fuzzy PID control strategy is adopted to adjust the temperature of the ball screw shaft by adjusting the coolant flow through the valve controlled hydraulic system. The relationship between temperature rise and flow is indirectly established without the disturbance of the heat generated in the cooling process. Immanuel et al. [5] curbed the temperature fluctuation by increasing the thermal inertia of the ball screw. The design of a paraffin-based phase change heat storage device for ball screw nut is introduced. The thermal measurement results show that the thermal inertia of ball screw increases during the process of paraffin melting and solidification. Moreover, the thermal resistance network and test-bed are used to study the heat storage element theoretically and experimentally. The model is built to assess the thermal behavior of the ball screw assembly to lay foundation for the prospective design of heat storage device. Ge et al. [6] availed of the thermal shrinkage of carbon fiber reinforced plastic (CFRP) to inhibit the thermal elongation of metal spindle housing. In the designed control system, the CFRP rods are evenly distributed around the spindle housing and the thermoelectric module (TEM) acts as a heat pump to transfer heat from the spindle housing to the CFRP rod. Compared with motorized spindle without thermal error control system, this method can reduce97% thermal displacement. The previous studies imply that although effective cooling and thermal insulation measures have been taken for the heat source, the cost has not been taken into account. Through the optimization analysis, the influence of heat source on ball screw can be minimized based on a certain cost and it is a necessity in actual production.

Thermal error modeling is the main content of thermal error compensation to ball screw, such as finite element modeling, neural network modeling and so on. Li et al. [7] combined the finite element method with Monte Carlo method on the basis of the finite element calculation data and used the exponential function of feed speed and time to describe the change of temperature difference between the measured surface point and the center of moving pair with time. In addition to that, an adaptive real-time model (ARTM) is constructed to predict the temperature transient distribution and thermal error distribution of ball screw shaft. Xu et al. [8] established the thermal characteristic model of the ball screw based on the finite element analysis and the improved lumped heat capacity method, and obtained the heating and heat dissipation equations of the bearing and ball screw nut pair. The temperature distribution, thermal deformation and air-cooling performance are simulated with the application of the established model. According to the comparative experiments, these methods can well predict the thermal behavior and air-cooling performance of ball screw pair system. Yang and Ni [9] used the dynamic neural network model to track the nonlinear time-varying machine tool errors under various thermal states. In order to adapt to the non-stationarity of thermoelastic processes, an integrated recurrent neural network (IRNN) is introduced to identify the non-stationarity of thermoelastic processes which presents a deterministic linear trend. The thermal error of the machine tool is [0, 50] μm before

compensation and it can be further reduced to [- 7,6] μm after compensation. Gao et al. [10] established a data-driven model based on LSTM neural network according to the collected time series data. The super parameters of LSTM neural network are optimized by PSO, and the PSO-LSTM model is established to ensure the accuracy of the prediction of the thermal error of ball screw pair. Based on the summary of the previous modeling methods, it can be found that high-precision prediction can be achieved, but it does not explore the specific contribution of different heat sources to the thermal error of the system in-depth. Heat source is the essential reason for the thermal behavior of ball screw. Quantifying the relationship between thermal error and heat source will contribute to the higher compensation accuracy.

Through the above analysis, it can be inferred that in previous studies, thermal error modeling could not quantify the impact of heat source, and that cooling measures could not balance the relationship between effect and cost. In view of the above problems, this paper analyzes the heat source contribution of the ball screw feed system from the following three aspects: theoretical analysis, thermal deformation modeling and heat source contribution optimization. On the basis of mathematical analysis, combined with neural network modeling, the expression of heat source contribution is obtained and the specific relationship between heat source and ball screw thermal deformation is also made clear. Moreover, the particle swarm optimization algorithm is used to obtain the optimal heat source contribution distribution. Finally, the accuracy of the optimization results is verified by simulation, as shown in **Fig. 1**.

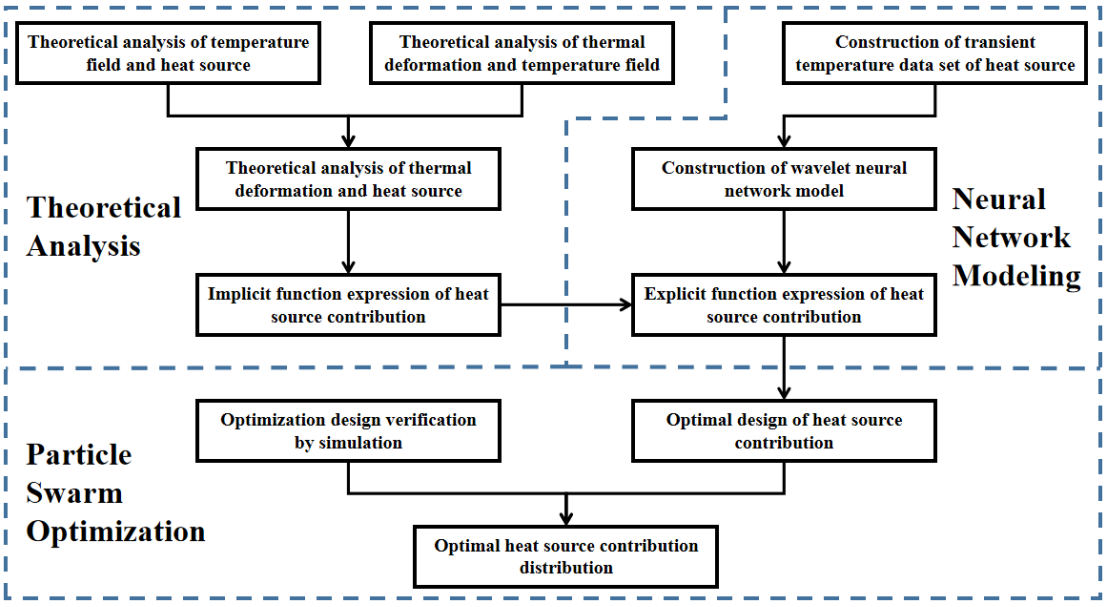

Fig. 1. Flow chart of heat source contribution analysis

1. Theoretical analysis of heat source contribution of ball screw

Heat source is the root cause of temperature field. The relationship between heat source and temperature is analyzed theoretically, and then the relationship between temperature and thermal deformation is analyzed so as to reveal the relationship between heat source and thermal deformation. On the other hand, the determination of the contribution of each heat source to the thermal deformation of the ball screw can help provide theoretical guidance for thermal error modeling.

1.1 Theoretical solution of the transient temperature rise of ball screw

Part of the heat generated by the heat source within a certain period of time improves the internal energy of the ball screw, whereas the other part vanishes by means of convective heat exchange with the surrounding medium. Based on this basic principle, the effects such as ball screw are transformed into a two-dimensional model, and the following heat balance equation can be listed [11]:

$$kQt = \rho cS\int_0^L T(x,t)dx + \int_0^t \int_0^L 2\pi rhT(x,t)dxdt \tag{1}$$

Where k is the proportional coefficient, Q is the heat source, and kQ is the heat transferred into the ball screw per unit time. ρ is the density, c is the specific heat capacity, S is the cross-sectional area of the ball screw, L is the length of the ball screw, t is the heat generation time of the heat source, r is the radius, h is the convective heat transfer coefficient between the ball screw and the surrounding medium, and $T(x,t)$ is the temperature distribution of the ball screw.

Let

$$G(t) = \int_0^L T(x,t)dx \tag{2}$$

Get

$$kQt = \rho cSG(t) + 2\pi rh\int_0^t G(t)dt \tag{3}$$

Take the derivative of t on both sides of **Eq. (3)** and obtain

$$kQ = \rho cSdG(t)/dt + 2\pi rhG(t) \tag{4}$$

By solving differential **Eq. (4)** and obtain

$$G(t) = kQ/2\pi rh - Cexp(-2\pi rht/\rho cS) \tag{5}$$

Where C is the undetermined constant.

Combining **Eq. (1)** and **Eq. (5)**, the average temperature rise of the ball screw concerning the heat source Q is

$$T(t) = kQ/2\pi rhL - Cexp(-2\pi rht/\rho cS) \tag{6}$$

The relationship between temperature and heat source can be seen at any time, as shown in **Fig. 2**.

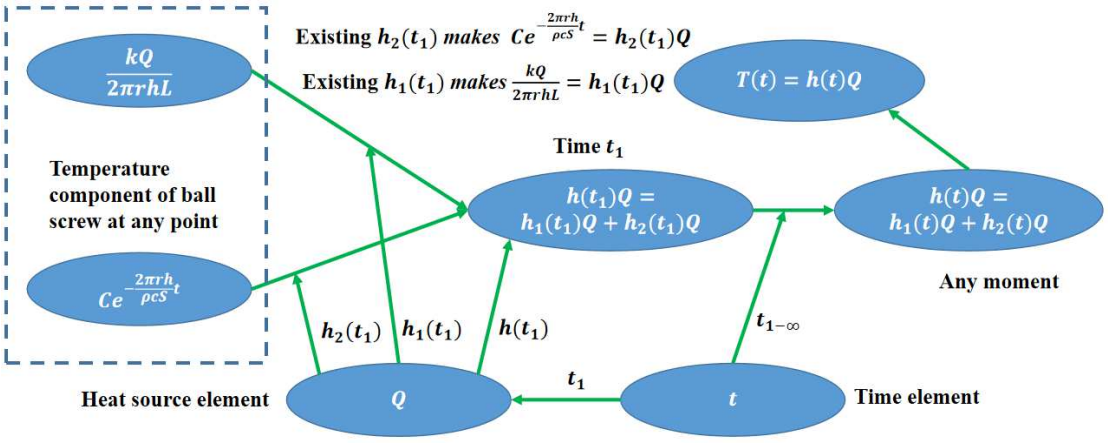

Fig. 2. Corresponding relationship between heat source and temperature

Let

$$kQ/2\pi rhL - Cexp(-2\pi rht/\rho cS) = h(t)Q \tag{7}$$

Get

$$T(t) = h(t)Q \tag{8}$$

Regarding the ball screw, there are four heat sources: motor, floating bearing, fixed bearing and ball screw nut pair, each of which is an independent heat source. According to the superposition principle of temperature field, the average temperature rise of ball screw is

$$T_S(t) = T_1(t) + T_2(t) + T_3(t) + T_4(t) \tag{9}$$

Where $T_S(t)$ is the temperature distribution under the comprehensive influence of each heat source at time t. $T_i(t)$ is the temperature distribution generated by the heat source Q_i at that time, $i = 1{\sim}4$.

Combine **Eq. (8)** and **Eq. (9)** to obtain

$$T_S(t) = h_1(t)Q_1 + h_2(t)Q_2 + h_3(t)Q_3 + h_4(t)Q_4 \tag{10}$$

Through the above analysis, the relationship between the temperature field of the ball screw and each heat source can be presented, as shown in **Eq. (10)**.

1.2 Theoretical solution of the heat source contribution degree of ball screw

Since the temperature rise $T(x,t)$ at any point x and the thermal deformation ΔL of the ball screw meet the following relationship [12]:

$$\Delta L = \int_0^x \alpha T(x,t)dx \tag{11}$$

For the convenience of research, the total thermal deformation ΔL_S of the ball screw is analyzed. At this time, the total deformation of the ball screw is:

$$\Delta L_S = \int_0^L \alpha T_S(x,t)dx \tag{12}$$

Where α is coefficient of thermal expansion.

Combine **Eq. (9)** and **Eq. (12)** to obtain

$$\Delta L_S = \alpha L\big(T_1(t) + T_2(t) + T_3(t) + T_4(t)\big) \tag{13}$$

Combine **Eq. (8)** and **Eq. (13)** to obtain

$$\Delta L_S = \alpha L(h_1(t)Q_1 + h_2(t)Q_2 + h(t)Q_3 + h_4(t)Q_4) \tag{14}$$

Namely

$$\Delta L_S = (Q_1, Q_2, Q_3, Q_4) \cdot \big(\alpha L h_1(t), \alpha L h_2(t), \alpha L h_3(t), \alpha L h_4(t)\big)^T \tag{15}$$

Let

$$\varepsilon(t) = \alpha L h(t) \tag{16}$$

$$Q = (Q_1, Q_2, Q_3, Q_4) \tag{17}$$

$$\varepsilon = \big(\varepsilon_1(t), \varepsilon_2(t), \varepsilon_3(t), \varepsilon_4(t)\big)^T \tag{18}$$

Where ε is the contribution matrix corresponding to the heat source Q, which reflects the effective effect of each heat source of the ball screw on the overall thermal deformation.

2.3 Optimization of heat source contribution of ball screw

In order to meet the needs of high-precision machining, adopting the method of cooling heat source is an effective way to reduce the thermal deformation of ball screw. Theoretically, the higher the cooling degree of the heat source, the smaller the thermal deformation. However, the higher the cooling degree of the heat source, the higher the corresponding cost. The contribution of the heat source reflects the effective influence of the heat source on the overall thermal deformation of the ball screw. If the heat source contribution is reduced, the effective influence of

the corresponding heat source on the thermal deformation and the thermal deformation will also be reduced. According to the above analysis, the contribution degree of heat source is a numerical expression of cooling degree. If the sum of the contribution of the heat source remains unchanged ($\varepsilon_1(t) + \varepsilon_2(t) + \varepsilon_3(t) + \varepsilon_4(t) = constant$), finding a set of contribution distributions ε that minimize ΔL_S cannot only the overall cooling degree and cost, but also effectively reduce the overall thermal deformation of the ball screw.

How to solve the heat source contribution matrix will be illustrated in detail in part 2. How to optimize the heat source contribution parameters will be described in detail in part 3.

2. Solution of heat source contribution based on WNN

This paper takes the X-axis ball screw of a horizontal machining center as the research object. Firstly, the transient temperature changes of ball screw motor, floating bearing, fixed bearing and ball screw nut heat source are measured. After that, the transient temperatures of the four heat sources are taken as the input variable and the thermal deformation of the ball screw are regarded as the output variable so as to contruct the neural network data set. Wavelet neural network (WNN) is used to build the prediction model of ball screw thermal error. After training, the relationship model between ball screw thermal error and four heat sources is established and the expression of heat source contribution under this working condition is deduced.

2.1 Data set construction

MT-X multi-channel temperature recorder is employed to measure the temperature change at each heat source of the ball screw. According to the movement law of the machine tool, the temperature measuring points are installed at the moving nut of the ball screw, the bearing seat at the fixed end, the bearing seat at the floating end and the motor surface without interfering with the movement of the machine tool, as shown in **Fig. 3**. The thermal error is measured by XL-80 laser interferometer. The variation trend of thermal error is the same as that of the temperature at the measuring point of the heat source, and the maximum thermal deformation is $34.5\mu m$ when the ambient temperature is $298.15K$.

It can be inferred from **Fig. 3** that the temperature at the motor is the highest, and that the steady-state temperature is $339.65K$; The fixed end bearing is close to the motor, so the temperature is greatly affected by the motor and the steady-state temperature is $316.15K$; The heat source of ball screw nut pair mainly comes from friction, and the steady-state temperature is $308.15K$; The bearing at the floating end has the lowest temperature, and the steady-state temperature is $305.35K$. The materials of the floating end bearing and the fixed end bearing are similar and their modes of heat generation are the same. Therefore, the actual temperature change should be similar. The influence of the motor on the fixed end bearing should be eliminated when solving the expression of the heat source contribution.

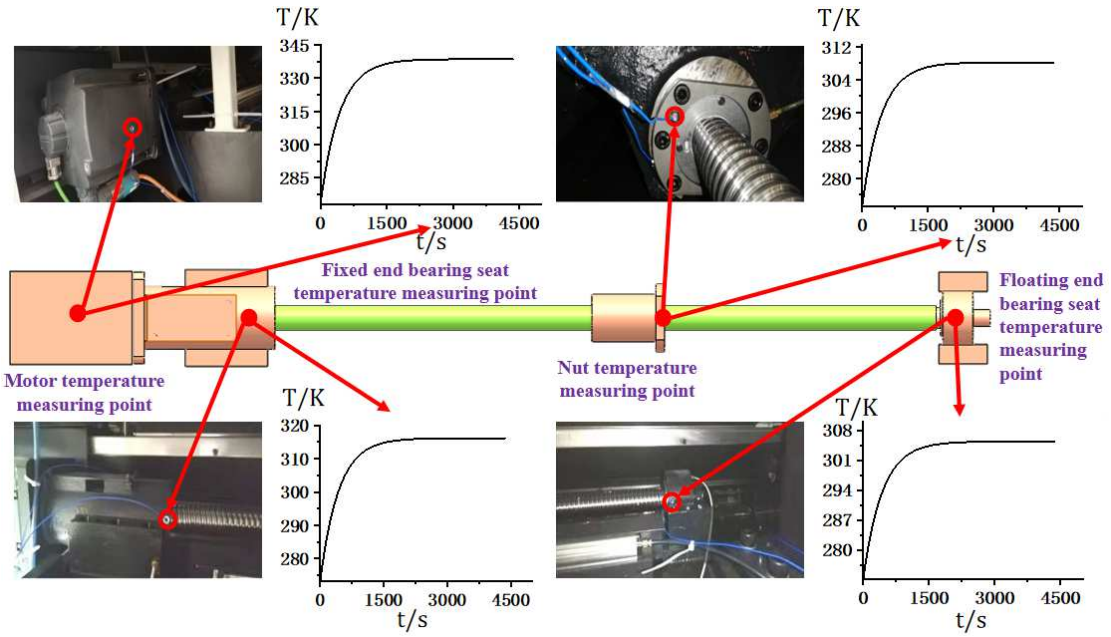

Fig. 3. Temperature rise of each heat source measuring point of ball screw

2.2 Construction of neural network model

Wavelet neural network (WNN) enjoys all the advantages of artificial neural network and wavelet analysis. It has the characteristics of fast convergence speed, avoiding falling into local optimization and those of time-frequency local analysis. Three-layer neural network can address any complex nonlinear problem [13]. Therefore, this paper establishes a three-layer WNN thermal error prediction model. The input of the model is the motor temperature rise, fixed end bearing temperature rise, floating end bearing temperature rise and nut temperature rise at time t, and the output is the predicted value of the overall thermal error of the ball screw at time t.

The total measurement time is 4358s and the total length of data is 4358. 4300 groups of data were randomly selected as the model training set, and the remaining 58 groups of data were used as the model test set. The network structure includes 4 nodes in the input layer, 15 nodes in the hidden layer and 1 node in the output layer.

Wavelet function is selected as the transfer function of input layer and hidden layer:

$$f(x) = \cos(1.75x)exp(-0.5x^2) \tag{19}$$

Sigmoid function is selected as the transfer function of hidden layer and output layer:

$$g(x) = 1/\big(1 + exp(-x)\big) \tag{20}$$

Input variable:

$$T = [T1 \quad T2 \quad T3 \quad T4]^T \tag{21}$$

Where $T1$ is the motor measuring point temperature, $T2$ is the fixed end bearing seat measuring point temperature, $T3$ is the floating end bearing seat measuring point temperature, and $T4$ is the nut measuring point temperature.

Relationship model of output variables and input variables [14]:

$$\Delta L_S = g(w \cdot f\big((v \cdot T + a + n)/m\big) + b) \tag{22}$$

Where ΔL_S is the overall thermal deformation of the lead screw at time t, n is the translation factor of the wavelet function, m is the shrinkage factor of the wavelet function, v is the weight of the input layer, w is the weight of the hidden layer, a is the threshold of the

hidden layer, and b is the threshold of the output layer.

Combine **Eq. (15)**, **Eq. (17)**, **Eq. (18)** and **Eq. (22)** and obtain

$$\Delta L_S(t) = g(w \cdot f\big((v \cdot \varepsilon(t) \cdot Q + a - n)/m\big) + b) \tag{23}$$

The contribution degree of heat source can be calculated by **Eq. (23)**

$$\varepsilon(t) = \Big(m \cdot f^{-1}\Big(\big(g^{-1}\big(\Delta L_S(t)\big) - b\big)/w\Big) - a + n\Big)/(vQ) \tag{24}$$

The training data is input to train the network model and the training iteration process is shown in **Fig. 4**(a). The model obtained after training is verified by the test data set, and the verification results are presented in **Fig. 4**(b). The average prediction error of neural network model is 4.4%. The weight, threshold, translation factor and contraction factor are extracted for the sake of the calculation of the contribution of heat source.

The weights from neural network input layer to hidden layer are shown in **Table 1**.

Table 1

Input layer to hidden layer weight

Weight v		Input layer nodes			
		1	2	3	4
Hidden layer nodes	1	0.76	0.53	0.42	0.26
	2	-0.09	0.47	-0.81	-0.84
	3	-0.06	0.48	-1.00	0.76
	4	0.24	-0.10	-0.13	0.34
	5	0.51	0.13	0.37	0.75
	6	-0.41	-0.09	0.41	-0.14
	7	-0.88	0.70	-0.70	0.78
	8	-0.60	-0.91	0.74	0.59
	9	0.78	0.09	0.30	-0.67
	10	0.69	0.69	-0.17	0.04
	11	0.37	-0.37	-0.24	-0.33
	12	-0.03	-0.69	-0.25	-0.61
	13	0.53	-0.95	0.51	-0.68
	14	0.68	-0.87	0.16	-0.66
	15	0.64	-0.46	0.12	0.55

The weights from hidden layer to output layer of neural network are shown in **Table 2**.

Table 2

Hidden layer to output layer weight

Type	Nodes and weights							
Hidden layer	1	2	3	4	5	6	7	8
Weight w	-0.66	-0.50	-0.03	1.06	-0.78	-1.53	0.32	0.02
Hidden layer	9	10	11	12	13	14	15	
Weight w	1.63	-0.14	1.57	0.72	0.04	0.74	-1.09	

The threshold from neural network input layer to hidden layer is shown in **Table 3.**

Table 3

Input layer to hidden layer threshold

Type	Nodes and thresholds							
Hidden layer	1	2	3	4	5	6	7	8
Threshold a	-0.75	-0.48	-0.44	0.52	-0.50	-0.32	-0.31	-0.88
Hidden layer	9	10	11	12	13	14	15	
Threshold a	0.18	0	0.39	-0.74	-0.60	-0.55	1.42	

The threshold from hidden layer to output layer of neural network is:

$$b = 0.89$$

The translation factor of wavelet function is shown in **Table 4**.

Table 4

Wavelet function translation factor

Type	Nodes and translation factors							
Hidden layer	1	2	3	4	5	6	7	8
Translation factors n	0.27	0.83	0.70	0.85	0.07	-0.06	0.72	0.29
Hidden layer	9	10	11	12	13	14	15	
Translation factors n	0.73	0.26	-0.06	0.28	0.91	0.41	0.42	

The shrinkage factor of wavelet function is shown in **Table 5.**

Table 5

Wavelet function shrinkage factor

Shrinkage factor m		Input layer nodes			
		1	2	3	4
Hidden layer nodes	1	0.67	0.68	0.70	0.70
	2	0.11	6.36	-2.45	-5.00
	3	0.49	0.51	0.46	0.52
	4	0.57	0.37	0.35	0.59
	5	0.75	0.59	0.77	0.86
	6	0.41	0.47	0.61	0.47
	7	0.17	0.16	0.17	0.16
	8	0.60	0.61	0.55	0.55
	9	0.86	0.65	0.60	0.49
	10	0	0.01	0.08	0.06
	11	1.03	1.13	1.09	1.15
	12	0.85	0.83	0.90	0.80
	13	0.23	0.24	0.23	0.24
	14	0.19	-0.03	0.27	0.04
	15	1.35	1.37	1.37	1.34

Where the corresponding heat source matrix is

$$Q = (66W \quad 37W \quad 37W \quad 58W)$$

With the accomplishment of the network training, the weight and threshold at the fixed end bearing seat are separated to obtain the real weight and threshold of the fixed end bearing and

avoid the interference of the motor at the same time. With the help of **Eq. (24)** and function fitting method, the contribution degree of each heat source is obtained, as shown in **Fig. 4**(c).

$$\varepsilon_1(t) = 0.064/\left(1 + exp(-0.0007t)\right) - 0.032 \tag{25}$$

$$\varepsilon_2(t) = 0.368/\left(1 + exp(-0.0014t)\right) - 0.184 \tag{26}$$

$$\varepsilon_3(t) = 0.370/\left(1 + exp(-0.0012t)\right) - 0.185 \tag{27}$$

$$\varepsilon_4(t) = 0.644/\left(1 + exp(-0.0024t)\right) - 0.322 \tag{28}$$

$$\Delta L_S = Q\varepsilon(T) = (Q_1, Q_2, Q_3, Q_4,)\left(\varepsilon_1(t)\ ,\varepsilon_2(t)\ ,\varepsilon_3(t), \varepsilon_4(t)\right)^T \tag{29}$$

And then

$$\Delta L_S = \left(0.064/\left(1 + exp(-0.0007t)\right) - 0.032\right)Q_1 + \left(0.368/\left(1 + exp(-0.0014t)\right) - 0.184\right)Q_2 + \left(0.370/\left(1 + exp(-0.0012t)\right) - 0.185\right)Q_3 + \left(0.644/\left(1 + exp(-0.0024t)\right) - 0.322\right)Q_4 \tag{30}$$

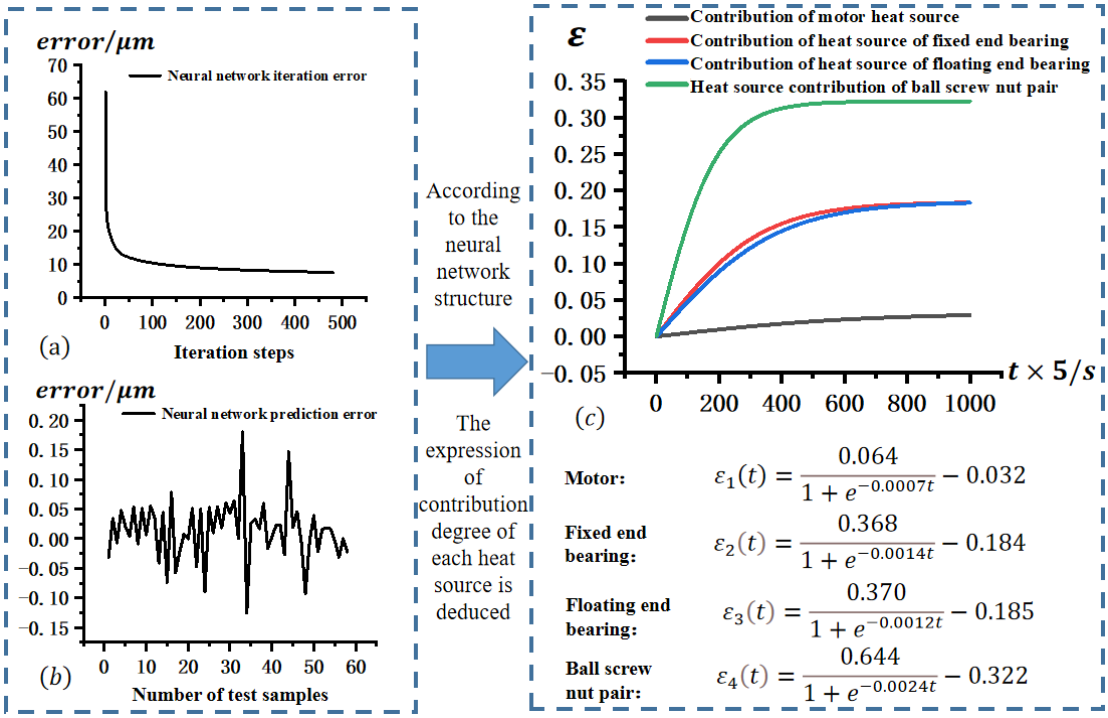

Fig. 4. Neural network training results and contribution results

The transient effect of different heat sources on the thermal deformation of the ball screw can be obtained using **Eq. (30)**, as shown in **Fig. 5**. As can be seen from **Fig. 5,** the heat source of the ball screw nut pair constitutes the largest proportion of the thermal deformation of the ball screw and the heat source of the fixed end bearing is similar to that of the floating end bearing in which the heat source of the motor is the smallest.

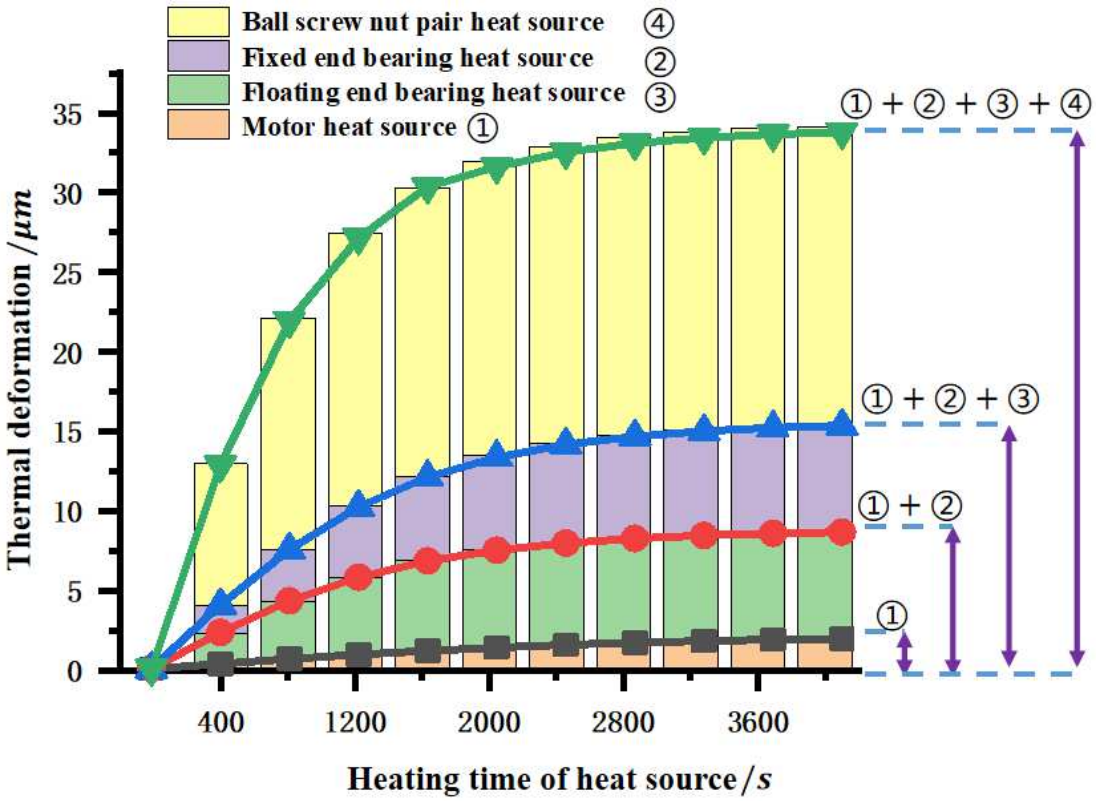

Fig. 5. Thermal deformation of ball screw under the influence of various heat sources

3. Optimization of heat source contribution based on PSO

Based on the above analysis, the transient expression of the contribution of each heat source to the thermal deformation of the ball screw is obtained. Keeping the total contribution of each heat source at a certain time of the ball screw unchanged, the optimal contribution distribution is calculated so as to minimize the thermal deformation of the ball screw at that time. Finally, the accuracy of the optimal distribution of the contribution of the heat source is verified by simulation analysis.

3.1 Optimization of heat source contribution

As the machine tool has a preheating process during the actual machining process, only the steady-state thermal deformation ($\Delta L_{S\infty}$) of the ball screw has an impact on the machining error. Therefore, the contribution of heat source in steady state is taken for optimization analysis. The relationship between the thermal deformation of the ball screw and each heat source in the steady state can be obtained by combining **Eq. (30)**.

$$\Delta L_{S\infty} = 0.032Q_1 + 0.184Q_2 + 0.185Q_3 + 0.322Q_4 \tag{31}$$

Particle swarm optimization algorithm enjoys fast search speed and high efficiency [15]. Particle swarm optimization algorithm is selected to find the optimal contribution distribution. The initial particle number is 50, the particle dimension is 4-dimensional, the inertia weight is 0.8, and the learning factor is 0.5. Taking the heat source as the constant value and the contribution degree as the variable, the fitness function is constructed with the combination of **Eq. (31)**. The constraint conditions are set as follows as shown in **Eq. (32)** to **Eq. (36).**

$$\varepsilon_1 + \varepsilon_2 + \varepsilon_3 + \varepsilon_4 = 0.032 + 0.184 + 0.185 + 0.322 = 0.7230 \tag{32}$$

$$0.3 \times 0.032 \leq \varepsilon_1 \leq 1.7 \times 0.032 \quad (33)$$
$$0.3 \times 0.184 \leq \varepsilon_2 \leq 1.7 \times 0.184 \quad (34)$$
$$0.3 \times 0.185 \leq \varepsilon_3 \leq 1.7 \times 0.185 \quad (35)$$
$$0.3 \times 0.322 \leq \varepsilon_4 \leq 1.7 \times 0.322 \quad (36)$$

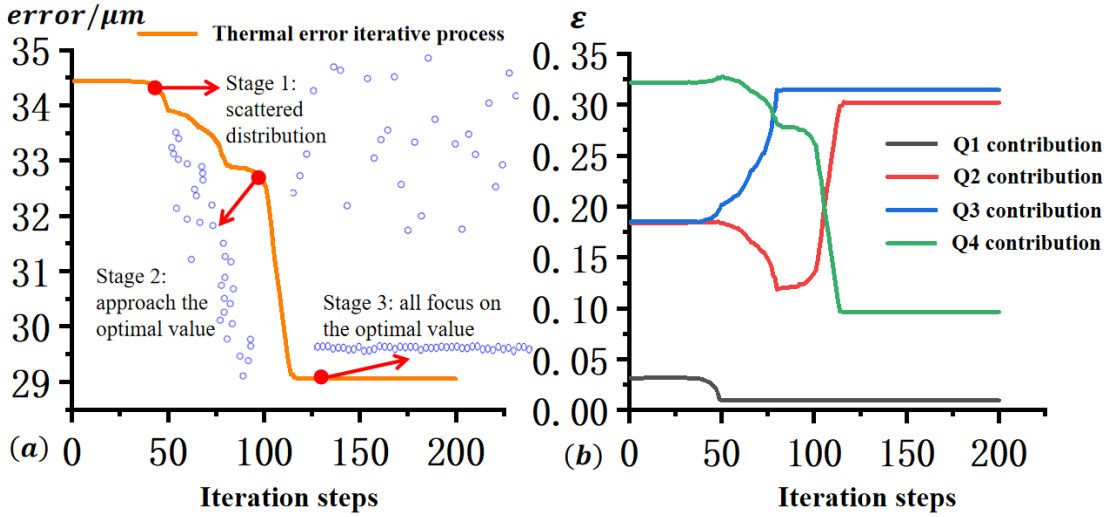

Fig. 6. Particle swarm optimization results

The particle swarm optimization process is shown in **Fig. 6**(a). The optimization process can be divided into three stages. The particles are scattered in the initial stage, close to the optimal value in the middle stage, and all particles focus on the optimal value in the later stage. The four dimensions of particles represent the contribution of four heat sources. The change process of the global optimal position of particles is illuminated in **Fig. 6**(b). It is noticeable that in the optimization process, the contribution of motor heat source and ball screw nut pair heat source declines gradually, and that the contribution of fixed end bearing heat source and floating end bearing heat source climbs gradually.

The optimized results are:

$$\varepsilon_1 = 0.00960$$
$$\varepsilon_2 = 0.31061$$
$$\varepsilon_3 = 0.30619$$
$$\varepsilon_4 = 0.09660$$
$$\Delta L_{S\infty} = 29.058\mu m$$

Thermal error reduction value of optimized heat source contribution distribution:

$$e = (34.5 - 29.058)/34.5 \times 100\% = 15.8\%$$

3.2 Simulation verification of optimization results

In order to verify the accuracy of particle swarm optimization results, the optimized heat source contribution distribution is simulated and analyzed, and the thermal deformation of ball screw under this distribution is calculated. For the convenience of the simulation, the change of the contribution degree of the heat source is converted into the change of the intensity of the heat source.

The conversion result is:

$$Q_1' = 0.0096 \times 66/0.032 = 19.8W$$
$$Q_2' = 0.31061 \times 37/0.184 = 62.5W$$

$$Q_3' = 0.30619 \times 37/0.185 = 61.2W$$
$$Q_4' = 0.0966 \times 58/0.322 = 17.4W$$

The thermodynamic parameters of the main material of the ball screw are given in **Table 6**.

Table 6

Thermodynamic parameters of ball screw material

Material	Density	Thermal conductivity	Specific heat capacity	Modulus of elasticity	Poisson's ratio	Coefficient of thermal expansion
45 steel	7850 $\mathrm{Kg/m^3}$	39.2 $\mathrm{W/(m \cdot K)}$	485 $\mathrm{J/(Kg \cdot K)}$	140 GPa	0.27	1.1×10^{-5} $\mathrm{K^{-1}}$

The corresponding load, boundary conditions and thermal resistance are set to simulate the temperature field. In order to simplify the simulation, the ambient temperature is set to the steady-state ambient temperature value (25℃). Taking the experimental data of temperature field as the standard, the temperature field simulation is corrected. Combined with the optimized data, the load imposed by the simulation, boundary conditions and ambient temperature are shown in **Table 7**.

Table 7

Simulation loads and boundary conditions

Parameters	Value
Heat generation rate of motor	$19.8W$
Heat generation rate of fixed end bearing	$62.5W$
Heat generation rate of floating end bearing	$61.2W$
Heat generation rate of lead screw nut pair	$17.4W$
Heat transfer coefficient of motor	$\mathrm{80W/(m^2 \cdot K)}$
Heat transfer coefficient of fixed bearing seat	$\mathrm{50W/(m^2 \cdot K)}$
Heat transfer coefficient of floating bearing seat	$\mathrm{55W/(m^2 \cdot K)}$
Nut heat transfer coefficient	$\mathrm{22W/(m^2 \cdot K)}$
Heat transfer coefficient of ball screw	$\mathrm{110W/(m^2 \cdot K)}$

The simulation results before optimization are shown in **Fig. 7**(a). At this time, the temperature at the nut is the highest and concentrated in one place, whereas the temperature field of the ball screw is unevenly distributed. The rise of thermal deformation is sharp with the maximum thermal deformation reaching $34.5\mu m$; the simulation results after optimization are shown in **Fig. 7**(b). At this time, the bearing temperature at both ends is higher than that of the nut temperature, with the maximum temperature not concentrated in one place. Nevertheless, the temperature field distribution is uniform compared with that before optimization. The rise of thermal deformation is gentler than that before optimization with the maximum thermal deformation reaching $29.5\mu m$. The simulation analysis indicates that the temperature field generated by the optimal heat source contribution distribution reduces the distribution gradient of ball screw thermal deformation and the maximum thermal deformation at the same time. The difference between the maximum simulated thermal deformation after optimization and the maximum thermal deformation after particle swarm optimization is $0.5\mu m$. Therefore, the optimization result is accurate.

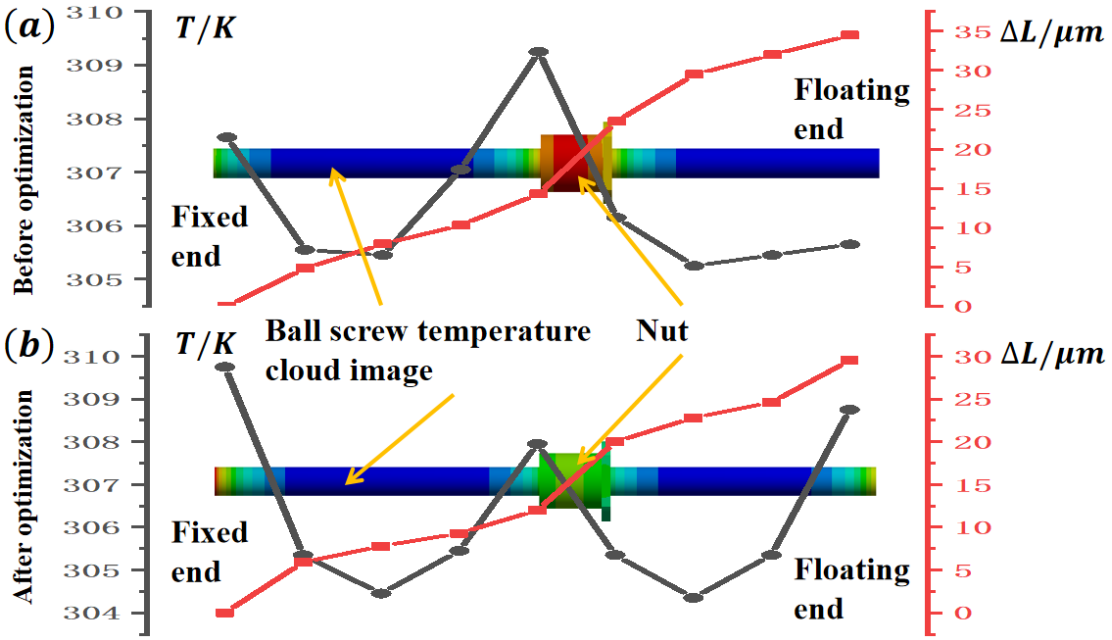

Fig. 7. Comparison of simulation results before and after optimization

Conclusions

The fundamental reason for the characteristics of thermal deformation and the distribution of temperature field is the distribution of heat source. The previous ball screw thermal error model does not fully reflect the role of heat source, and there is a contradiction between the poor cooling effect and the high cost of each heat source in the system. In view of the above problems, the contribution of each heat source of the ball screw feed system to the overall thermal error is studied, and the relationship between the cooling effect and the cooling cost is balanced by optimizing the contribution. Based on the results and analysis, the following conclusions can be drawn:

(1) This paper proposes a calculation method of heat source contribution based on wavelet neural network, sets up the neural network model of ball screw thermal deformation about each heat source and obtains the functional expression of heat source contribution. Finally, the quantitative relationship between the thermal deformation of ball screw and each heat source under specific working conditions is clarified.

(2) The contribution distribution of each heat source in steady state is analyzed by particle swarm optimization algorithm. Keeping the total contribution of each heat source unchanged, a set of optimal contribution distributions with the minimum thermal deformation are determined to address the contradiction between the poor cooling effect and the high cooling cost and make full use of the cooling resources of the ball screw.

(3) The temperature field distribution and thermal deformation characteristics of the ball screw before and after optimization are simulated and analyzed. The temperature field distribution of the ball screw after optimization is more uniform than that before optimization, and the thermal deformation gradient is significantly reduced. The comparison of the simulated thermal deformation under the optimal contribution distribution with the algorithm optimized thermal deformation proves the accuracy of the particle swarm optimization results.

Acknowledgements

This research is supported by Jiangsu Science and Technology Achievement Conversion Project (No.BA2018093). It is great thankful to NEWAY CNC EQUIPMENT（SUZHOU）CO., LTD.

References

[1] Mayr J, Jedrzejewski J, Uhlmann E, et al. Thermal issues in machine tools[J]. CIRP Annals - Manufacturing Technology, 2012, 61(2):771–791.

[2] YANG J，SHI H，FENG B，et al. Thermal error modeling and compensation for a high-speed motorized spindle[J]. The International Journal of Advanced Manufacturing Technology，2015，77(5-8)：1005-1017.

[3] ZHAO Liang, WANG Mengchao, LEI Mohan, et al. A Differentiated Active Cooling Strategy for Feed Axis of Precision Boring Machine[J]. JOURNAL OF XI'AN JIAOTONG UNIVERSITY, 2022, 56(2):10.

[4] Shi H, He B, Yue Y, et al. Cooling effect and temperature regulation of oil cooling system for ball screw feed drive system of precision machine tool[J]. Applied Thermal Engineering, 2019, 161:114150-114150.

[5] Voigt I, NDS Iñaki, Wermke B, et al. Increased thermal inertia of ball screws by using phase change materials[J]. Applied Thermal Engineering, 2019, 155:297-304.

[6] GE Zeji, DING Xiaohong. Design of thermal error control system for high-speed motorized spindle based on thermal contraction of CFRP[J]. The International Journal of Advanced Manufacturing Technology, 2018, 125:99-111.

[7] Li T J, Zhao C Y, Zhang Y M. Adaptive real-time model on thermal error of ball screw feed drive systems of CNC machine tools[J]. International Journal of Advanced Manufacturing Technology, 2018, 94(2):1-9.

[8] Xu Z Z, Liu X J, Kim H K, et al. Thermal error forecast and performance evaluation for an air-cooling ball screw system[J]. International Journal of Machine Tools & Manufacture, 2011, 51(7-8):605-611.

[9] YANG H, NI J. Dynamic neural network modeling for nonlinear, nonstationary machine tool thermally induced error - ScienceDirect[J]. International Journal of Machine Tools and Manufacture, 2005, 45(4–5):455-465.

[10] Gao X, Guo Y, Hanson D A, et al. Thermal Error Prediction of Ball Screws Based on PSO-LSTM[J]. International Journal of Advanced Manufacturing Technology, 2021, 116(5-6):1721-1735.

[11] Mei, Xuesong, Zhao, et al. Investigation into effect of thermal expansion on thermally induced error of ball screw feed drive system of precision machine tools[J]. International Journal of Machine Tools & Manufacture, research and application, 2015, 97:60-71.

[12] Huang S, Feng P, Xu C, et al. Utilization of heat quantity to model thermal errors of machine tool spindle[J]. International Journal of Advanced Manufacturing Technology, 2018, 97(5-8):1733-1743.

[13] HAYKIN S, NETWORK N. A comprehensive foundation[J]. Neural networks, 2004, 2(2004):41.

[14] Bin L I, Zhang Y, Wang L, et al. Modeling for CNC Machine Tool Thermal Error Based on Genetic Algorithm Optimization Wavelet Neural Networks[J]. Journal of Mechanical Engineering, 2019, 55(21):215-220.
[15] Kahya M, Ozbayoglu M, Unver H O. Precision and energy-efficient ball-end milling of Ti6Al4V turbine blades using particle swarm optimization[J]. International Journal of Computer Integrated Manufacturing, 2021, 34(2):110-133.

Statements and Declarations

Funding

This research is supported by Jiangsu Science and Technology Achievement Conversion Project (No.BA2018093).

Competing Interests

The authors have no relevant financial or non-financial interests to disclose.

Author Contributions

All authors contributed to the study conception and design. Theoretical analysis, model building and optimization analysis were performed by [Huayang Wu], [Jiejing Li] and [Dunwen Zuo]. The first draft of the manuscript was written by [Huayang Wu] and all authors commented on previous versions of the manuscript. All authors read and approved the final manuscript.